Desorption Processes: Supercritical Fluid Regeneration of Activated Carbon

Models are developed for isothermal desorption in a fixed bed of adsorbent particles. While more general models require numerical solution of the governing equations, two practically important cases have analytical solutions: 1) an equilibrium desorption model where the rate of desorption is controlled by external and intraparticle mass transfer; and 2) a kinetic model where external and intraparticle mass transfer and a first-order irreversible desorption step control the overall process.

Recent experimental data (Tan and Liou, 1988) for the desorption of ethyl acetate from activated carbon with supercritical carbon dioxide are found to fit the local-equilibrium model. Data for the effect of temperature on fractions desorbed indicate a reversal of the temperature dependence of the adsorption isotherm as the supercritical pressure is increased. This phenomenon is analogous to the observed cross-over region for the effect of temperature on the solubility of a solid at supercritical conditions.

F. Recasens
B. J. McCoy
J. M. Smith
Department of Chemical Engineering
University of California
Davis, CA 95616

Introduction

Desorption processes, except for the temperature-programmed type, have received little attention. Desorption of gases from fixed beds of porous particles has been analyzed with various models as part of predicting the performance of pressure-swing-adsorption (PSA) cycles (Ruthven 1984; Yang, 1987). Doong and Yang (1986) developed two types of mathematical treatments:

1) An equilibrium model wherein concentrations in the bulk fluid are in equilibrium with uniform adsorbed concentrations

2) A surface and pore diffusion model that assumes equilibrium at a desorption site but includes intraparticle concentration gradients

Recently, Shin and Knaebel (1987, 1988a) and Matz and Knaebel (1988) employed a pore-diffusion model combined with experimental data to explain the effects of operating conditions and design variables on the performance of PSA. In all cases equilibrium has been assumed at one or another location. To our knowledge, there is no literature for cases where adsorption-desorption kinetics can affect results. This may be important in some examples of PSA as noted by La Cava et al. (1988) in a recent presentation. The several differential equations, needed to explain the complete cycle of PSA, require numerical solution.

Our objectives are twofold.

1. To develop models for desorption from fixed beds of porous particles—models that include finite rates for both the desorption step at a site and the mass transfer processes.
2. To identify the model that best fits recent experimental data (Tan and Liou, 1988) for the desorption of ethyl acetate from activated carbon with supercritical carbon dioxide

Regeneration of adsorbents with supercritical carbon dioxide is advantageous because it can be carried out at much lower temperatures than thermal regeneration. In addition, the thermal process normally must be followed with gasification and accompanying carbon loss, if complete regeneration is to be obtained (Chihara and Smith, 1981). The first treatment of supercritical regeneration appears to be the research of de Filippi et al. (1980) and Modell et al. (1979) who presented experimental data and information on process development. The data of Tan and Liou (1988), however, provide published information in enough detail to use for evaluating rate models.

First, we give the governing equations for a general case where axial dispersion, external and intraparticle mass transfer, and nonlinear kinetics can influence overall desorption rates. Then analytical solutions are derived for: 1) a two-parameter model where mass transfer and first-order irreversible kinetics control the process; and 2) a two-parameter model based upon desorption equilibrium existing at an interior desorption site and mass transfer. For both solutions the linear-driving force concept is used so that a modest amount of intraparticle diffusion resistance as well as external (particle to fluid) mass transfer can be included. The effects of temperature and flow rate observed by Tan and Liou (1988) fit the equilibrium desorption model. Our analysis shows that both intraparticle diffusion and external mass transfer retard the desorption rate. At low supercritical pressures a reverse isotherm is indicated, analogous to the decrease in solubility with temperature increase observed in the supercritical region. Also, the results for high supercritical pressures suggest the existence for desorption of a cross-over region similar to that observed for solubility.

General Model

Consider a packed bed of spherical adsorbent particles with an initial loading of adsorbate of concentration C_{a_0}. Pure solvent fluid is introduced to the bed, which operates isothermally. It is first assumed that the adsorption is of the non-linear Langmuir form. Initially the solvent rapidly fills the pores of the particles. For these conditions mass conservation equations for the adsorbate in the void region, in the pores, and on the particles, are

$$\alpha \frac{\partial C}{\partial t} + u \frac{\partial C}{\partial z} = E \frac{\partial^2 C}{\partial z^2} - \frac{3(1-\alpha)k_m}{r_0}[C - (C_i)_{r=r_0}] \quad (1)$$

$$\beta \frac{\partial C_i}{\partial t} = D_e \frac{1}{r^2}\frac{\partial}{\partial r}\left(r^2 \frac{\partial C_i}{\partial r}\right) - \rho k_a (C_m - C_a) C_i + \rho k_d C_a \quad (2)$$

$$\frac{\partial C_a}{\partial t} = k_a (C_m - C_a) C_i - k_d C_a \quad (3)$$

with boundary and initial conditions

$$D_e \left(\frac{\partial C_i}{\partial r}\right)_{r=r_0} = k_m [C - (C_i)_{r=r_0}] \quad (4)$$

$$\left(\frac{\partial C_i}{\partial r}\right)_{r=0} = 0 \quad (5)$$

$$C(r, z, t=0) = C_i(r, z, t=0) = 0 \quad (6)$$

$$C_a(r, z, t=0) = C_{a_0} \quad (7)$$

$$C(r, z=0, t) = 0 \quad (8)$$

These equations can be solved numerically for the effluent concentration $C(L, t)$ and the fraction desorbed as a function of time. The results would be general in that kinetics of desorption-adsorption at a site are included as well as intraparticle diffusion, fluid-particle mass transfer, and axial dispersion. In certain cases one or more of these individual processes would not affect the fraction desorbed and in some instances analytical solutions are possible, as shown in the following sections.

Special Cases

Linear kinetics

The adsorption rate terms in Eqs. 2 and 3 are for adsorbed concentrations less than corresponding to monolayer coverages and as such are second order. As complete desorption is approached C_a becomes small with respect to the monolayer concentration C_m. Then, Eqs. 2 and 3 are linear

$$\beta \frac{\partial C_i}{\partial t} = D_e \left(\frac{1}{r^2}\right) \frac{\partial}{\partial r}\left(r^2 \frac{\partial C_i}{\partial r}\right) - \rho k'_a C_i + \rho k_d C_a \quad (9)$$

$$\frac{\partial C_a}{\partial t} = k'_a C_i - k_d C_a \quad (10)$$

where $k'_a = k_a C_m$.

Irreversible desorption

For this case, Eq. 10 reduces to

$$-\frac{\partial C_a}{\partial t} = k_d C_a \quad (11)$$

and Eqs. 2 and 3 again become linear.

Approximation for intraparticle diffusion (Linear driving force model)

Much of the numerical effort in solving the general case, Eqs. 1–8 is caused by the interactions necessary to solve Eq. 2 with boundary conditions given by Eqs. 4 and 5. Do and Rice (1986) showed that assuming a parabolic concentration profile within the particle is an excellent approximation for equilibrium adsorption when $t > 0.05(\beta + K)r_0^2/D_e$, i.e., for all but very small values of time. For calculation of moments in dynamic diffusion-reaction systems, Tomida and McCoy (1987) have shown that the assumption of a parabolic intraparticle concentration profile is a very good approximation for Thiele modulus (ϕ) values less than 2 and a reasonable one for somewhat higher values. The Thiele modulus is defined as

$$\phi = r_0 (\rho k / D_e)^{1/2} \quad (12)$$

With the parabolic profile assumption, intraparticle diffusion and external mass transfer effects can be contained in an overall coefficient k_p (the linear driving force model),

$$k_p = 5k_m \Big/ \left(5 + \frac{k_m r_0}{D_e}\right) \quad (13)$$

With k_p, Eq. 2 can be written in terms of an average concentration $\bar{C}_i$

$$\beta \frac{\partial \bar{C}_i}{\partial t} = \frac{3k_p}{r_0}(C - \bar{C}_i) - \rho k_a (C_m - \bar{C}_a)\bar{C}_i + \rho k_d \bar{C}_a \quad (14)$$

Average intraparticle concentrations are evaluated using the parabolic profile $C(r)$ in the following equation

$$\bar{C} = \frac{1}{\frac{4}{3}\pi r_0^3} \int_0^{r_0} 4\pi r^2 C(r)\, dr \quad (15)$$

Replacing Eq. 2 with Eq. 14 greatly simplifies the solution and in some cases leads to analytical rather than numerical results. In terms of average concentrations Eqs. 1 and 3 become

$$\alpha \frac{\partial C}{\partial t} + u \frac{\partial C}{\partial z} = E \frac{\partial^2 C}{\partial z^2} - \frac{3(1-\alpha)k_p}{r_0}(C - \overline{C}_i) \tag{16}$$

$$\frac{\partial \overline{C}_a}{\partial t} = k_a(C_m - \overline{C}_a)\overline{C}_i - k_d \overline{C}_a \tag{17}$$

Equilibrium

If the adsorbed and fluid concentrations are in equilibrium at an interior site and for a linear adsorption isotherm

$$C_a = KC_i \tag{18}$$

where

$$K = k_a'/k_d \tag{19}$$

Now Eq. 18 replaces Eq. 3.

If intraparticle diffusion is accounted for by the linear driving force model, Eq. 14, Eq. 18 is replaced with

$$\overline{C}_a = K\overline{C}_i \tag{20}$$

Analytical Solutions

In many cases two-parameter models should be adequate to explain observed desorption data from fixed beds. For example, in long beds axial dispersion is usually negligible. When intraparticle concentration gradients are not severe the linear driving force model is satisfactory for combining external and intraparticle mass transfer effects. If, in addition, first-order kinetics is applicable, Eqs. 16, 14 and 9 become

$$\alpha \frac{\partial C}{\partial t} + u \frac{\partial C}{\partial z} = -\frac{3(1-\alpha)k_p}{r_0}(C - \overline{C}_i) \tag{21}$$

$$\beta \frac{\partial \overline{C}_i}{\partial t} = \frac{3k_p}{r_0}(C - \overline{C}_i) - \rho k_a' \overline{C}_i + \rho k_d \overline{C}_a \tag{22}$$

$$\frac{\partial \overline{C}_a}{\partial t} = k_a' \overline{C}_i - k_d \overline{C}_a \tag{23}$$

Finally, the desorption rate will sometimes be irreversible so that $\rho k_a' \overline{C}_i$ in Eq. 22 in negligible and Eq. 23 becomes

$$\frac{\partial \overline{C}_a}{\partial t} = -k_d \overline{C}_a \tag{24}$$

Equations 21, 22 and 24 define a two-parameter (k_p and k_d) irreversible desorption kinetic model. In other instances the adsorption-desorption process may be very fast so that equilibrium is approached. Then, Eq. 20 with Eqs. 22 and 23 define an equilibrium model with k_p and K as parameters.

Analytical solutions can be obtained for these two-parameter models. The initial and boundary conditions for the equilibrium case are

$$C(z=0,t) = C(z,t=0) = 0 \tag{25}$$

$$\overline{C}_a(z,t=0) = C_{a_0} \tag{26}$$

and, in addition, for the irreversible desorption case

$$\overline{C}_i(z,t=0) = 0 \tag{27}$$

Equilibrium desorption

Combining Eqs. 22 and 23 to eliminate the k_a' and k_d, and using Eq. 20 to remove $\overline{C}_i$, yields

$$(\rho + \beta/K)\frac{\partial \overline{C}_a}{\partial t} = \frac{3k_p}{r_0}(C - \overline{C}_a/K) \tag{28}$$

This expression, and Eqs. 21, 25 and 26, define the equilibrium case with parameters k_p and K. It is supposed that equilibrium in the pores is established instantaneously so that the initial concentration of adsorbate in the pore liquid is C_{a_0}/K. If the adsorption equilibrium constant is measured independently, this model has but one parameter, the overall mass transfer coefficient. The solution may be found by Laplace transformation, inverting the transform of C with the convolution integral (Recasens, 1988). The results for $C/(C_{a_0}/K)$ in the bed effluent are:

For $\theta \leq 1$ [$0 \leq t \leq$ (one residence time)]

$$\frac{C(L,t)}{C_{a_0}/K} = \frac{b'}{b+b'}[1 - \exp[-(b+b')\theta]] \tag{29}$$

For $\theta > 1$

$$\begin{aligned}\frac{C(L,t)}{C_{a_0}/K} = \frac{b'}{b+b'}&\exp[-(b+b')\theta][\exp(b+b') - 1] \\ &+ \exp[-(b+b')(\theta - 1)] \\ &\cdot \sum_{m=0}^{\infty}(-1)^{m+1}\left(\frac{b}{b'}\right)^m \frac{A_m(b')A_m[b'(1-\theta)]}{(m!)^2}\end{aligned} \tag{30}$$

where

$$\theta = \frac{tu}{L\alpha} \tag{31}$$

$$b = \frac{3k_p L\alpha}{r_0(\beta + \rho K)u} \tag{32}$$

$$b' = \frac{3(1-\alpha)k_p L}{r_0 u} \tag{33}$$

and A_m is related to the incomplete gamma function:

$$A_m(w) = \int_0^w \exp(-\tau)\tau^m \, d\tau \tag{34}$$

which may be calculated from

$$\begin{aligned} A_0 &= 1 - \exp(-w); \quad m = 0 \\ A_m(w) &= A_{m-1}(w) - w^m \exp(-w); \quad m \geq 1 \end{aligned} \tag{35}$$

The fraction F of the total possible desorption is given by

$$F(\theta) = \frac{\int_0^{\theta} [C(L, t)/(C_{a_0}/K)]\, d\theta}{\int_0^{\infty} [C(L, t)/(C_{a_0}/K)]\, d\theta} \tag{36}$$

With Eqs. 29 and 30, the fractions desorbed are

For $\theta \leq 1$

$$F = \frac{b}{b + b'} \left\{ \theta - \frac{1}{b + b'} (1 - \exp[-(b + b')\theta]) \right\} \tag{37}$$

For $\theta > 1$

$$\begin{aligned} F = {} & \frac{b}{b + b'} \left[1 - \frac{\exp[-\theta(b + b')][\exp(b + b') - 1]}{b + b'} \right] \\ & + \frac{1}{b + b'} \sum_{m=0}^{\infty} \frac{A_m(b') A_m[b(\theta - 1)]}{(m!)^2} \\ & - \frac{b}{(b + b')b'} \exp[-(b + b')(\theta - 1)] \\ & \cdot \sum_{m=0}^{\infty} (-1)^{m+1} \left(\frac{b}{b'}\right)^m \frac{A_m(b') A_m[b'(1 - \theta)]}{(m!)^2} \end{aligned} \tag{38}$$

Irreversible desorption

Equations 21, 22 (with $\rho k'_a \overline{C}_i \rightarrow 0$), and 24 with Eqs. 25–27 define the problem of irreversible desorption with parameters k_p and k_d. The solution for the effluent concentration, obtained as before, by Laplace transformation and convolution, is

For $\theta \leq 1$

$$\frac{C(L, t)}{C_{a_0}\rho} = \frac{b'(Da/\beta)}{b_0 + b' - Da} \left\{ \frac{1}{Da} [1 - \exp(-Da\theta)] - \frac{1}{b_0 + b'} [1 - \exp[-\theta(b_0 + b')]] \right\} \tag{39}$$

For $\theta > 1$

$$\frac{C(L, t)}{C_{a_0}\rho} = \frac{b'(Da)}{b'[1 + \alpha/\beta(1 - \alpha) - Da]} \left(\frac{G_1 - G_2}{\beta} \right) \tag{40}$$

where

$$\begin{aligned} G_1 = {} & \frac{\exp(-Da\theta)}{Da} [\exp(Da) - 1] + \exp[-Da(\theta - 1)] \\ & \cdot \sum_{m=0}^{\infty} \frac{(-1)^{m+1} b_0^m A_m(b') A_m[(b_0 - Da)(\theta - 1)]}{(Da - b_0)^{m+1} (m!)^2} \end{aligned} \tag{41}$$

$$\begin{aligned} G_2 = {} & \frac{\exp[-(b_0 + b')\theta]}{b_0 + b'} \\ & [\exp(b_0 + \mathrm{b}') - 1] + \exp[-(b_0 + b')(\theta - 1)] \\ & \cdot \sum_{m=0}^{\infty} \frac{(-1)^m b_0^m A_m(b') A_m[b'(1 - \theta)]}{(b')^{m+1} (m!)^2} \end{aligned} \tag{42}$$

and

$$Da = \frac{k_d \alpha L}{u} \tag{43}$$

$$b_0 = \frac{3 k_p L \alpha}{r_0 \beta u} \tag{44}$$

If the desorption rate is very large, $Da/b_0 \rightarrow \infty$, mass transfer controls the overall process and Eqs. 39 and 40 reduce to

$$\frac{C(L, t)}{C_{a_0}\rho} = \frac{1 - \exp(-\theta(b_0 + b')]}{\beta\alpha + (1 - \alpha)}, \quad \text{for } \theta \leq 1 \tag{45}$$

$$\frac{C(L, t)}{C_{a_0}\rho} = \frac{b' G_2}{\beta}, \quad \text{for } \theta > 1 \tag{46}$$

The solution for this case is independent of k_d.

At the other extreme the desorption rate controls the process ($Da/b_0 \rightarrow 0$). Then $G_2 \rightarrow 0$ and the solution becomes

$$\frac{C(L, t)}{C_{a_0}\rho} = \frac{(1 - \alpha)[1 - \exp(-Da\theta)]}{\alpha + \beta(1 - \alpha)}, \quad \text{for } \theta \leq 1 \tag{47}$$

$$\frac{C(L, t)}{C_{a_0}\rho} = \frac{(1 - \alpha)[\exp(-Da\theta][\exp(-Da) - 1]}{\alpha + \beta(L - \alpha)}, \quad \text{for } \theta > 1 \tag{48}$$

Integrating Eqs. 39 and 40 gives analytical expressions for the fraction desorbed for the irreversible desorption model.

Model Discrimination

The most general model described by Eqs. 1–8 includes the effects of five rate processes, represented by rate constants E, k_m, D_e, k_a, k_d. As usual, axial dispersion can be eliminated if the Peclet number, $L\,u/E$, is large, and the significance of external mass transfer depends upon the flow rate. The conventional way of determining whether or not the model should include intraparticle diffusion is to make experiments with different size particles. An alternate calculational approach is to assume the linear driving force model and evaluate k_p from data for one particle size. If k_p is significantly less than k_m, calculated from available correlations (for example, Wakao and Kaguei, 1982), intraparticle transport affects the overall process.

The prior equations show that modeling is simplified if the desorption is irreversible. This can best be determined by independent measurement of the adsorption isotherm. Also, the isotherm establishes the range of concentrations for which first-order kinetics are applicable. If desorption is reversible, but k_a and k_d are sufficiently large that equilibrium is achieved at a desorption site, these rate constants are replaced by K. Data on fraction, F, desorbed at different temperatures can in some instances help discriminate between equilibrium or kinetic models. If F increases as temperature increases, no such discrimination is possible provided desorption is the usual endothermic process. Both desorption equilibrium constant and desorption rate constant increase with temperature. In contrast, if fractions desorbed decrease as T increases, an equilibrium model is suggested. An irreversible kinetic model would give negative activation energy. Such experimental behavior has been observed in the supercritical region (Tan and Liou, 1988) implying that an equilibrium model, rather than a desorption rate model, should be used. If equilibrium is assumed this kind of data suggests exothermic desorption.

Analysis of Ethyl Acetate Desorption from Activated Carbon

The recent data (Tan and Liou, 1988) for ethyl acetate desorption with supercritical CO_2 provide an opportunity for modeling desorption processes. Fractions desorbed from a fixed bed of carbon particles were measured for various flow rates at 328 K and 8.83 MPa(T_r = 1.08, P_r = 1.18 for CO_2). Fractions desorbed were also determined from 300 K to 338 K (T_r = 0.99 to 1.11) at two pressure levels 8.83 MPa P_r = 1.18) and 13.1 MPa (P_r = 1.75). All measurements were with 18–20 mesh activated carbon particles for which the average particle diameter is 1.0×10^{-3} m.

In choosing a model for correlating these results, it is noted first that the fractions desorbed increased with flow rate (Figure 1). This suggests that the model should include external mass transfer (k_m). For 1×10^{-3} m particles which contain small pores, e.g., activated carbon, intraparticle diffusion may well retard the overall rates. Since data for different particle sizes are unavailable an approximate approach is to use the linear driving force model to evaluate k_p. Such results can then be compared with literature correlations for k_m to see if intraparticle diffusion resistance is significant.

The data show that at the lower pressure, 8.83 MPa, the fraction desorbed (for the same time) decreases as the temperature increases. As noted in the prior section this suggests that equilibrium may exist between adsorbed and fluid concentrations at a desorption site. At a pressure (13.1 MPa) considerably above the critical value for CO_2, there is relatively little effect of temperature. Comparison with solubility results at supercritical conditions may explain this unusual behavior. Figure 2 for the solubility of napthalene in carbon dioxide [McHugh and Paulaitis (1980), Kander and Paulaitis (1983)] shows that at relatively low supercritical pressures, for example at 8 MPa, the solubility decreases as the temperature increases between 300 and 325 K. At higher supercritical pressures (12 MPa) the solubility is nearly unchanged in this temperature region. At still higher pressures the solubility increases with T, corresponding to the normal endothermic process. This reversal with pressure of solubility of a solute is the same phenomenon as observed by Tan and Liou.

This qualitative analysis of the data suggests that a promising model should include external and intraparticle mass transfer and be based upon equilibrium at a desorption site. Adsorption isotherms at the temperatures and pressures involved, and data for at least one other particle size, would have been helpful to confirm these conclusions. The available information suggests that the two-parameter (k_p and K) equilibrium model, culminating in Eqs. 37 and 38, be used to analyze the experimental data.

Effect of flow rate

The desorption experiments of Tan and Liou (1988) were carried out in a 2.1×10^{-2}m ID column packed with the 18–20 mesh particles. The initial ethyl acetate loading was 1.97×10^{-3} kmol/kg[0.15 kg/(kg of carbon)]. The points in Figure 1 for the fraction desorbed represent their data and indicate a strong effect of flow rate except for the two lowest velocities. Tan and

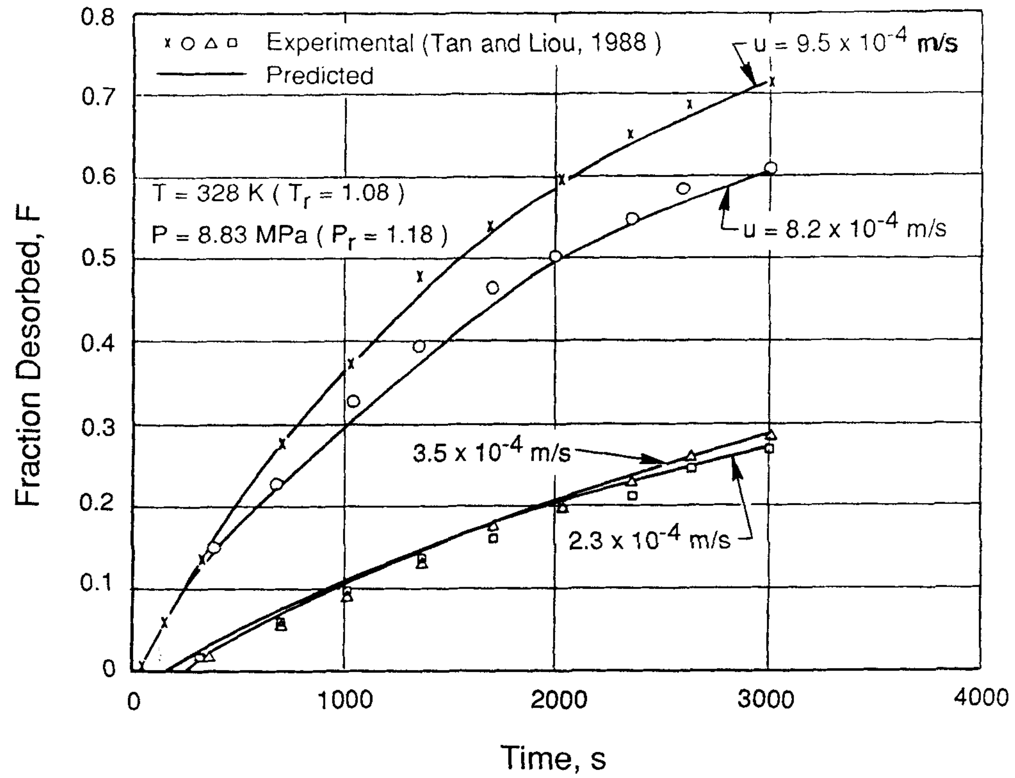

Figure 1. Effect of CO_2 flow rate on fraction desorbed.

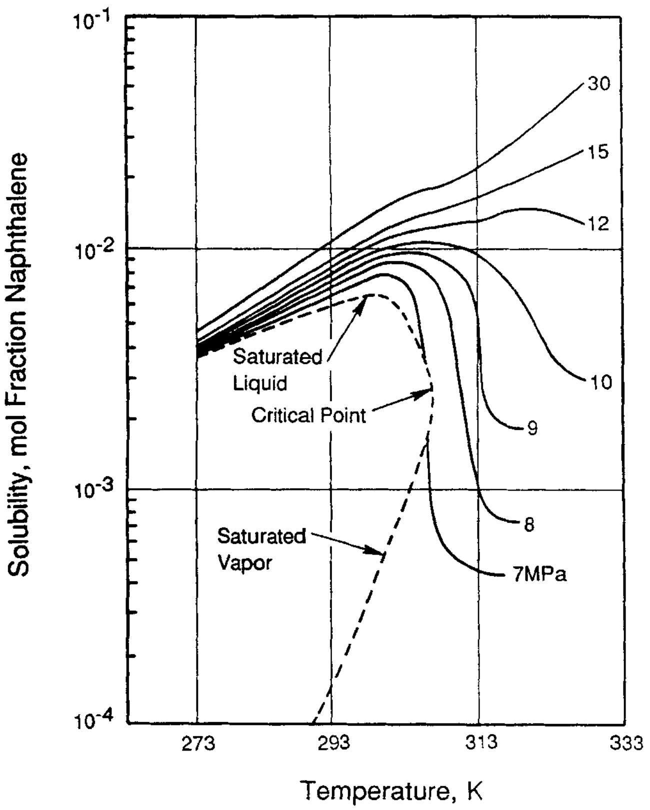

Figure 2. Solubility of naphthalene in supercritical carbon dioxide.

From McHugh and Paulaitis (1980) and Kander and Paulaitis (1983)

Table 1. Adsorption Equilibrium Constants *K* and Overall Mass Transfer Coefficients k_p (T = 328 K, P = 87.1 atm)

Velocity, u* m/s × 10^4	Kp	$k_p \times 10^4$ m/s	$D_e \times 10^8$ m²/s	$k_m \times 10^4$** m/s
9.5	12	0.73	0.95	3.1
8.2	14	0.65	0.83	2.9
3.5	17	0.29	0.35	2.0
2.3	16	0.18	0.20	1.7

*Superficial velocities, u, are at desorber temperature and pressure.
**k_m values are from Wakao and Kaguei (1982), Eq. 49.

Liou mention that at long times the data for $u = 3.5 \times 10^{-4}$ m/s showed larger fractions desorbed than that for $u = 2.3 \times 10^{-4}$ m/s.

Optimal values of k_p and K were obtained by visual comparison of data points and curves calculated from Equation (38). The curves were evaluated and displayed, using TK Solver Plus on an IBM PC-AT computer with graphics capability. Since the experiments were at constant temperature and pressure, K should have the same value at all flow rates. However, k_p will change. A starting value for k_p was obtained by calculating k_m from the Wakao and Kaguei correlation

$$\frac{2r_0k_m}{D} = 2 + 1.1\left(\frac{2r_0u\rho}{\mu}\right)^{0.6}\left(\frac{\mu}{\rho D}\right)^{1/3} \qquad (49)$$

and estimating the viscosity and density according to the recommendations of Reid et al. (1987). D was estimated to be 3.9×10^{-8} m²/s by the method of Takanashi (1974). These property values gave a Schmidt number of 2.2. At the beginning of the

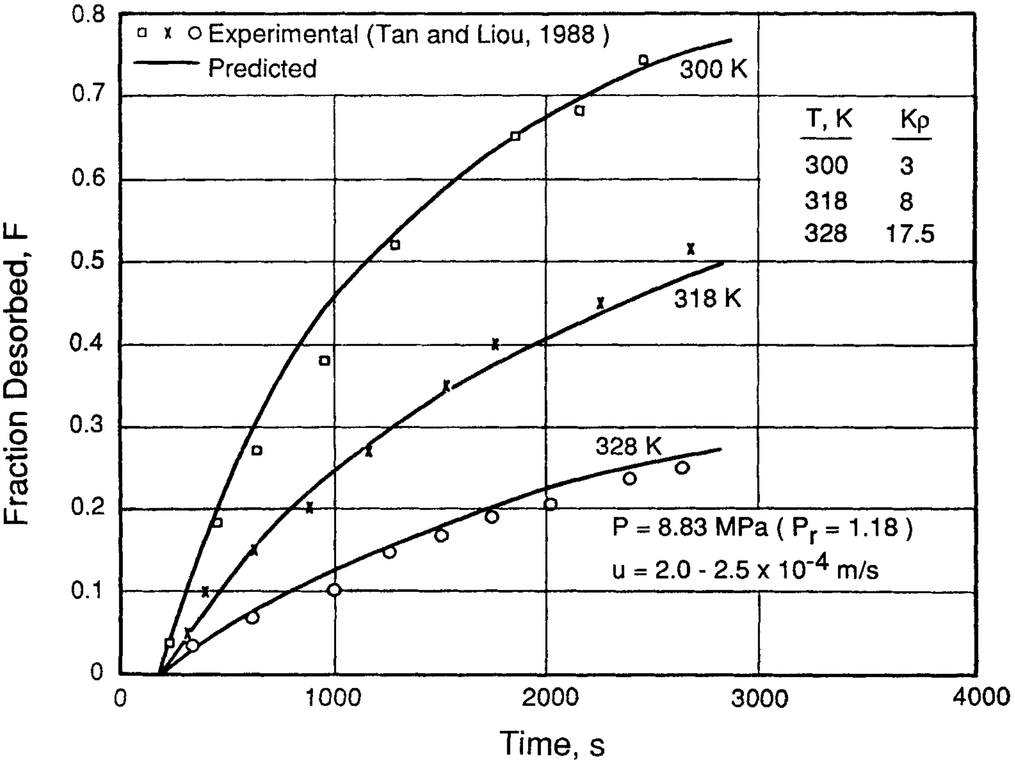

Figure 3. Effect of temperature on fraction desorbed at low supercritical pressure (P_r = 1.18).

optimization, D was approximated by taking the tortusoity factor δ $(= \beta D/D_e)$ equal to $1/\beta$ (Wakao and Smith, 1962). Then k_p was obtained from Eq. 13. From then on the optimization was continued leading to the final values of $K\rho$ and k_p given in Table 1. The final computed results, shown by the continuous curves in Figure 3 agree well with the experimental points. The criterion of Do and Rice (1986),

$$t > 0.05\,(\beta + K\rho)r_0^2/D_e \tag{50}$$

provides a conservative estimate of 3 min as the time beyond which the linear driving force model should be accurate.

The sensitivity of the computed curves to K was much greater than to D_e. Therefore, k_p, and hence D_e, cannot be as accurately determined as K. The variation of D_e (Table 1), which is a very sensitive quantity, does not significantly affect K. The $K\rho$ values in Table 1, which ideally should be identical, vary from 12 to 17. However, the two largest values are for the two lowest velocities. The experimental results at these velocities are suspect since their curves in Figure 1 nearly coincide. One would expect a relatively large divergence at the lowest velocities. The k_p values are up to one order of magnitude less than k_m calculated from Eq. 49, demonstrating that intraparticle diffusion as well as external mass transfer affect the rate. Data for different particle sizes would be necessary along with the model described by Eqs. 1–8 in order to establish more accurate values of D_e. However, the diffusivity values in Table 1 are of the expected magnitude. With $D = 3.9 \times 10^{-8}$ m^2/s the tortuosity factor based upon an average value of D_e of 0.6×10^{-8} m^2/s is 4.

Effect of temperature

The experimental data of Tan and Liou (1988) on the effect of temperature are shown in Figure 3 by the experimental points. These results are for the lower supercritical pressure (8.83 MPa) and indicate that the fraction desorbed decreases markedly as the temperature increases. The flow rate measured at 298 K and 101.3 kPa was constant but varied from 0.2×10^{-3} to 0.95×10^{-3} m/s at desorber conditions. The solid curves in Figure 3 were calculated from Eqs. 37 and 38. The overall mass transfer coefficient k_p given in Table 1 for the lowest velocity is applicable except for the effect of temperature. The small corrections were made by taking into account the effect of temperature on D_e and k_m and using Eq. 13. Hence, the only variable in the curve-fitting procedure is $K\rho$ and the optimum values for each temperature are also given in Figure 3. The $K\rho$ results are shown on a van't Hoff plot in Figure 4 and give an approximate heat of adsorption, $\Delta H = 50$ kJ/mol, based upon K expressed in concentrations. This unconventional behavior is analogous to the reverse solubility behavior shown in Figure 2 for the lower supercritical pressures.

At the higher supercritical pressure (13.1 MPa), the measurements of Tan and Liou show little effect of temperature (from 300 to 328 K). Hence, the values of $K\rho$ were nearly constant and varied from 3 to 3.3 as shown also in Figure 4. The pressure at which the effect of temperature on solubility reverses has been termed the crossover point (Chimowitz and Pennisi, 1986; Schaeffer et al. 1988). Our results for $K\rho$ indicate that a similar crossover pressure exists for desorption and that for ethyl acetate desorbing from activated carbon into CO$_2$ this pressure is near 13 MPa.

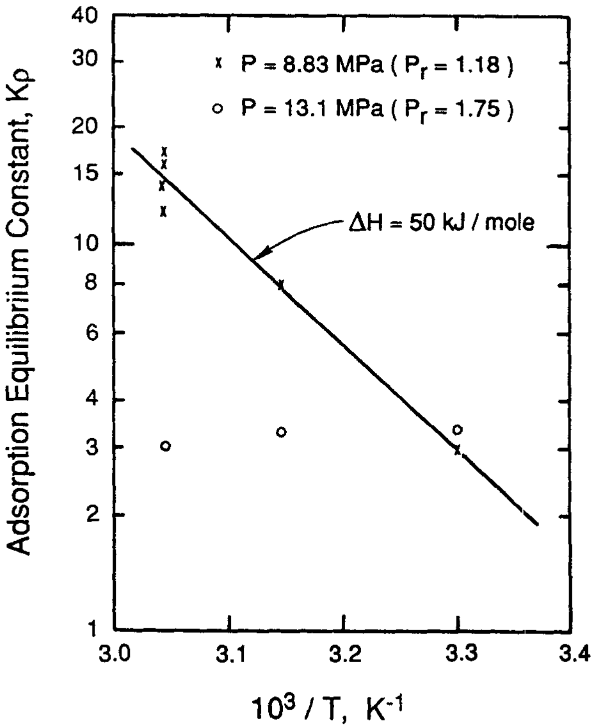

Figure 4. Adsorption equilibrium constants at low and high supercritical pressures.

Acknowledgment

The fellowship support of the Spain-U.S. Committee for Scientific and Technological Cooperation and financial support of National Science Foundation Grant (NSF Grant #CBT-8700092) are gratefully acknowledged.

Notation

$A_m(w)$ = incomplete gamma function, defined by Eqs. 49–51
b, b', b_0 = dimensionless groups defined by Eqs. 32, 33 and 44
C = concentrations of adsorbate in bulk fluid, kmol/m^3
$\bar{C}$ = average
C_a = adsorbed concentration, kmol/kg
C_{a_0} = initial concentration
C_i = concentration in pores, kmol/m^3
C_m = monolayer adsorbed concentration, kmol/kg
D = molecular diffusivity, m^2/s
Da = Damkoehler number, Eq. 43
D_e = effective diffusivity in the porous particles, m^2/s
E = axial dispersion coefficient, m^2/s
F = fraction desorbed
G_1, G_2 = functions described by Eqs. 41 and 42
ΔH = approximate heat of adsorption, kJ/mol
K = adsorption equilibrium constant, m^3/kg
k = first-order adsorption rate constant, m^3/kg · s
k_a = second-order adsorption rate constant, m^6/kmol · s · kg
k_a' = pseudo first-order adsorption rate constant, m^3/kg · s
k_d = first-order desorption rate constant, L/s
k_m = external (particle-to-bulk fluid) mass transfer coefficient, m/s
k_p = overall mass transfer coefficient, Eq. 13, m/s
L = bed length, m
m = positive integers
P = pressure, MPA
P_c = critical pressure
P_r = reduced pressure, P/P_c
r = radial coordinate from center of particle
r_0 = particle radius

T = temperature, K
T_c = critical temperature
T_r = reduced temperature, T/T_c
t = time, s
u = superficial velocity at T and P of bed, m/s
z = bed length, m

Greek letters

α = bed void fraction
β = porosity of particles
δ = tortuosity factor = $\beta D/D_e$
ρ = density of particles, kg/m^3
θ = dimensionless time, Eq. 31
τ, w = dummy quantities, Eq. 49
ϕ = Thiele modulus, Eq. 12

Literature Cited

Chihara, K., and J. M. Smith, "Regeneration of Powdered Activated Carbon," *AIChE J.*, **27**, 213, 220 (1981).

Chimowitz, E. H., and K. J. Pennisi, "Process Synthesis Concepts for Supercritical Gas Extraction in the Cross-Over Region," *AIChE J.*, **32**, 1665 (1986).

de Filippi, R. P., V. J. Krukonis, R. J. Robey, and M. Modell., "Supercritical Fluid Regeneration of Activated Carbon for Adsorption of Pesticides," EPA Report 600/2-80-0511 (Mar., 1980).

Do, D. D., and R. G. Rice, "Validity of the Parabolic Profile Assumption in Adsorption Studies," *AIChE J.*, **32**, 149 (1986).

Doong, S. J., and R. T. Yang, "Bulk Separation of Multicomponent Gas Mixtures by Pressure Swing Adsorption: Pore/Surface Diffusion and Equilibrium Models," *AIChE J.*, **32**, 397 (1986).

Kander, R. G., and M. E. Paulaitis, "Chemical Engineering at Supercritical Fluid Conditions," M. E. Paulaitis, J. Penninger, R. Gray, and P. Davidson, eds., Ann Arbor Science, Ann Arbor, 461 (1983).

La Cava, A. I., J. A. Dominguez, and G. Cardenas, "Modeling Kinetically Induced PSA Separations," China-Japan-USA Symp. on Advanced Adsorption Separation Science and Technology, Hangzhou, China (Sept. 18–21, 1988).

Matz, M. J., and K. S. Knaebel, "Pressure Swing Adsorption: Effects of Incomplete Purge," *AIChE J.*, **34**, 1486 (1988).

McHugh, M. A., and M. E. Paulaitis, "The Solubility of Naphthalene and Biphenyl in Supercritical Carbon Dioxide," *J. Chem. Eng. Data*, **15**, 326 (1980).

Modell, M., R. J. Robey, V. Krukonis, R. P. de Filippi, and D. Oestreich, "Supercritical Fluid Regeneration of Activated Carbon," AIChE Meeting Boston (Aug., 1979).

Recasens, F., "Supercritical Fluid Regeneration of Spent Activated Carbon," Report on File at Department of Chemical Engineering, University of California, Davis (Sept., 1988).

Reid, R. C., J. M. Prausnitz, and B. E. Poling, "The Properties of Gases and Liquids," 4th ed., McGraw-Hill New York (1987).

Ruthven, D. M., "Principles of Adsorption and Adsorption Processes," Wiley, New York (1984)

Schaeffer, S. T., L. H. Zalkow, and A. S. Teja, "Supercritical Extraction of Crotalaria Spectabilis on the Cross-Over Region," *AIChE J.*, **34**, 1740 (1988).

Shin, H.-S., and K. S. Knaebel, "Pressure Swing Adsorption: A Theoretical Study of Diffusion-Induced Separations," *AIChE J.*, **33**, 654 (1987); "Pressure Swing Adsorption: An Experimental Study of Diffusion-Induced Separation," *ibid*, **34**, 1409 (1988a).

Takanashi, S., "Preparation of a Generalized Chart for the Diffusion Coefficients of Gases at High Pressures," *J. Chem. Eng. Japan*, **7**, 417 (1974).

Tan, C.-S., and D.-C. Liou, "Desorption of Ethyl Acetate from Activated Carbon by Supercritical Carbon Dioxide," *Ind. Eng. Chem. Res.*, **27**, 988 (1988).

Tomida, T., and B. J. McCoy, "Polynomial Profile Approximation for Intraparticle Diffusion," *AIChE J.*, **33**, 1908 (1987).

Wakao, N., and S. Kaguei, "Heat and Mass Transfer in Packed Beds," Gordon and Breach, Sci. Publications, New York (1982).

Wakao, N., and J. M. Smith, "Diffusion in Catalyst Pellets," *Chem. Eng. Sci.*, **17**, 825 (1962).

Yang, R. T., "Gas Separation by Adsorption Processes," Butterworths, Stoneham, MA (1987).

Manuscript received Dec. 13, 1988, and revision received Feb. 22, 1989.